Organic Petrological Characteristics of Graptolite and Its Contribution to Buried Organic Carbon of Longmaxi Formation Shales, Middle Yangtze Region

Wenhao Li [1,2,*], **Xiuzhe Wang** [1,2], **Min Wang** [1,2] **and Erqiang Yang** [1,2]

1   Shandong Provincial Key Laboratory of Deep Oil and Gas, China University of Petroleum (East China),
     Qingdao 266580, China; z19010191@s.upc.edu.cn (X.W.); wangm@upc.edu.cn (M.W.);
     s20010122@s.upc.edu.cn (E.Y.)
2   School of Geosciences, China University of Petroleum (East China), Qingdao 266580, China
*   Correspondence: liwh@upc.edu.cn

Abstract: The shale gas exploration of the Longmaxi Formation in the Yangtze Region of China has made a significant breakthrough. As an important hydrocarbon generation organism, graptolite is widely distributed in the Longmaxi Formation shales, but its hydrocarbon potential is still unclear. Taking the Longmaxi Formation shales in the Middle Yangtze Region as an example, this paper discusses the organic petrological characteristics of graptolite and its contribution to buried organic carbon. The Longmaxi shales in the study area can be divided into organic-rich shales (TOC > 2.0%) and organic-bearing shales (TOC < 2.0%). The organic-rich shales have high quartz content and low clay mineral content, which is opposite in the organic-bearing shales. Organic maceral results show that graptolite is widely distributed in nearly all the samples, while solid bitumen is relatively developed in organic-rich shale. The equivalent vitrinite reflectance obtained from the conversion of graptolite reflectance ranges from 2.46% to 2.76%, indicating that the organic matter maturity of the Longmaxi Formation shale is overmature. Combining an optical microscope and a field emission scanning electron microscope, the proportion of graptolite area to organic matter area can be obtained, the average of which is 32.71%. Solid bitumen mainly contributes to buried organic carbon of the organic-rich shales in the Longmaxi Formation, while graptolites contribute little to organic carbon burial. However, solid bitumen in the organic-bearing shales is relatively undeveloped, and graptolite is an important hydrocarbon generation organism, which is the main contributor to buried organic carbon.

Keywords: graptolite; hydrocarbon generation organism; buried organic carbon; maceral; Longmaxi Formation

1. Introduction

Graptolites are types of extinct colonial marine animals, which are widely distributed in the Ordovician and Silurian marine source rocks [1,2]. There is a set of graptolite-bearing shales in the Wufeng–Longmaxi Formations (Upper Ordovician-Silurian) with the maximum total organic carbon (TOC) values 10% [3] and which are the main source rocks and fossil hydrogen energy productive reservoir in the Yangtze region [4,5]. The study of the Longmaxi graptolite is mainly focused on biostratigraphy and the sedimentary environment [6–11]. The organic petrology characteristics of graptolites as well as the contribution of graptolite organic matter to organic carbon burial are still unclear due to the limited research on optical characteristics of graptolites and unrecognizable macerals of graptolite and other organic components in the optical microscope. Liu et al. [12] believed that the structural evolution of graptolite is mainly finished by deoxygenation, denitrification, and carburetion, and graptolite can be a significant hydrocarbon generation material in low maturity. When the maturity is low, the graptolite shows rich carboxyl,
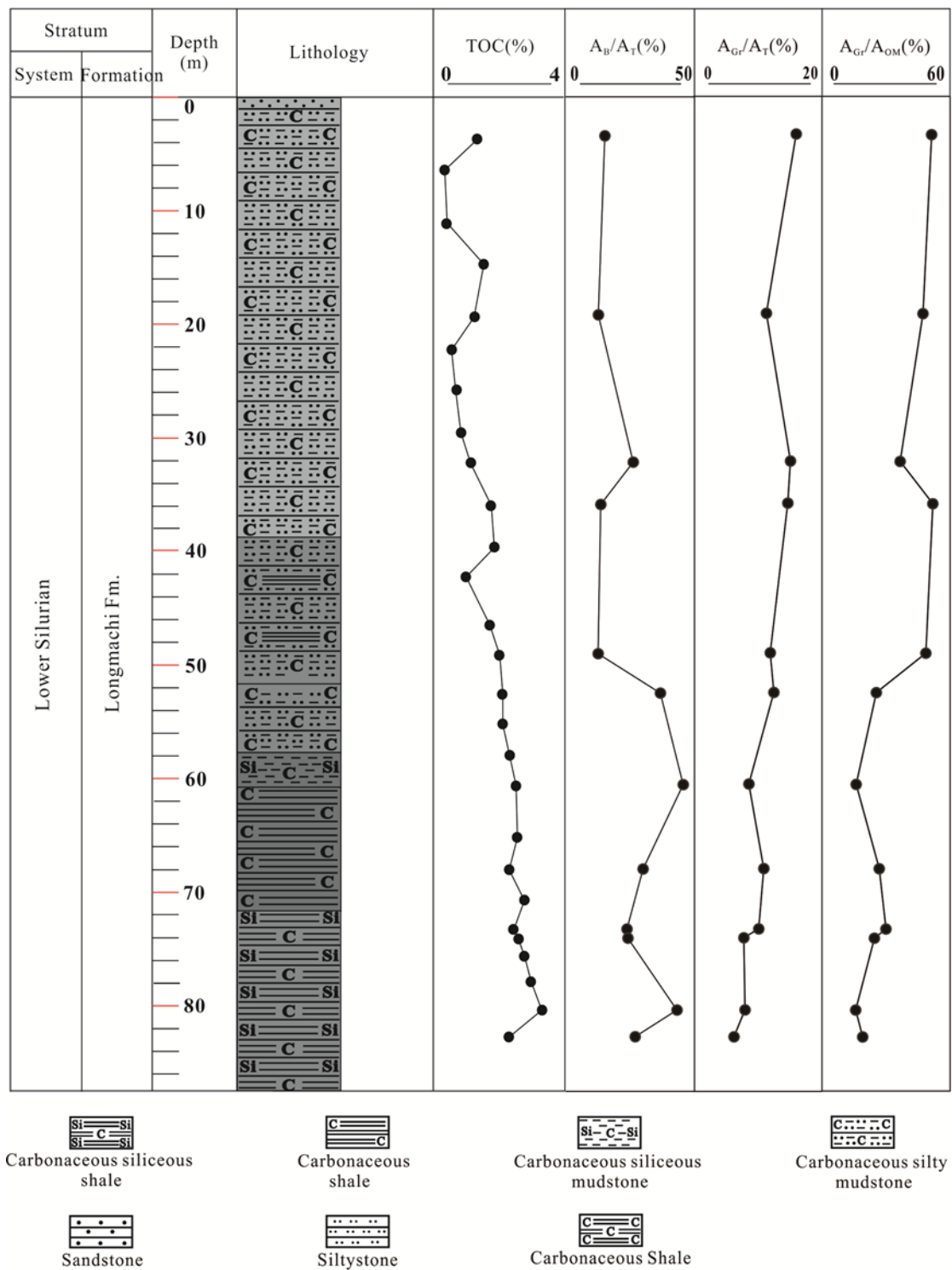
carbonyl, acyl functional groups, and poor aromatics. With the increase of maturity, the oxygen-containing functional groups in the graptolite's structure are reduced, and the cross-linked structures, such as oxygen bridges, are condensed, which may lead to the generation and accumulation of hydrocarbons. Luo et al. [2] discussed optical characteristics of graptolite in the Wufeng–Longmaxi shales and believed that graptolite epidermis have complex biogenetic structures and fusellar layers and are commonly filled by pyrites. The TOC values of shales have positive correlations with the diversity and organic matter abundance of graptolites [13], showing that graptolites have important contributions to buried organic carbon. A mass of organic pores of graptolite epidermis can be observed in scanning electron microscope (SEM) images, suggesting that graptolites are of great significance to hydrocarbon potential and reservoir space of shales [14]. However, there also exists the opposite view that the abundance of graptolite in the shales has no correlation with the TOC values, suggesting that graptolites have little contribution to organic matter enrichment [3].

The research on organic petrology characteristics of graptolites is limited, and the contribution of graptolite organic matter to organic carbon burial remains controversial. Thus, this paper discusses the optical characteristics of graptolites and reflectance of graptolites for organic matter maturity evaluation. The proportion of graptolite area to organic matter area was calculated by combining the optical microscope with the SEM, and the relationship between the proportion and the TOC values was discussed to reveal the contribution of graptolites to organic carbon burial in this paper.

2. Geological Background

The Central Yangtze area formed a stable platform after the Jinning Movement (1000–800 Ma). It has experienced the Caledonian, Hercynian, Indosinian, Yanshan, and Himalayan major tectonic movement transformations. The late Ordovician–Devonian developed foreland basins dominated by clastic deposits. The Middle Yangtze region accepted the muddy siliceous deposits formed in the anoxic environment. The study area is located in the Xianning area in the southeast of Hubei Province, Central Yangtze region (Figure 1). The strata in the Xianning area are well developed, and the Mesoproterozoic–Quaternary strata are exposed. The Nanhua System is divided into the Liantuo Formation, Gucheng Formation, Datangpo Formation, and Nantuo Formation from bottom to top. The Liantuo Formation is deposited by coarse to fine purplish-red clastic rocks from bottom to top. The Sinian is a stable platform in an epicontinental sea and shallow marine carbonate platform environment with low-velocity deposits, such as argillaceous limestone and carbonaceous shale. Later, it was transformed into an open sea platform to limited platform carbonate deposition. Phosphorus-bearing dolomite is often deposited in the slope area of the platform front. The Cambrian–Silurian system is dominated by dolomite in the restricted environment, which is partially exposed and subject to weathering and erosion. Longmaxi shales were deposited as part of a global early Silurian anoxic event [15]. The research area was a shallow sea shelf environment when the Lower Silurian Longmaxi Formation was deposited. A set of black and gray-black carbonaceous shale, siliceous shale and gray-green silty shale were deposited in the Longmaxi Formation, which is rich in graptolite and well preserved. Continental red clastic rocks were deposited in the Middle and Late Jurassic. A set of continuously continental red clastic rocks was deposited in the Cretaceous–Neogene. It is a complex sedimentary rock series with multiple centers, multiple provenances, and multiple rhythms.

Figure 1. Sampling sites from the Xikeng section in southeastern Hubei Province, China.

3. Samples and Methods

3.1. Sample Material

The Lower Silurian Longmaxi shale samples were collected from the Xikeng section in the Xianning area of southeastern Hubei Province, China (Figure 1). The Longmaxi Formation is characterized by a shelf environment with a thickness of 87.51 m (Figure 2). The bottom Longmaxi Formation is in conformable contact with the underlying gray–yellow sandstones of the upper Ordovician Huangnigang Formation. The lower Longmaxi Formation shale samples are rich in graptolite fossils. Some samples have visible dispersed pyrite and horizontal bedding. The samples are mainly black and ash black carbonaceous shale and carbonaceous siliceous shale. The upper section mainly develops silty mudstone mingled with carbonaceous shale. From bottom to top, the content of graptolite is reduced, the content of silt is increased, and the color becomes lighter (Figure 2). A total of 27 samples were collected in this study.

Figure 2. Stratigraphic columns of the Longmaxi Formation from the Xikeng section in southeastern Hubei Province, China. A_B/A_T: absolute values of bitumen area/total horizon area; A_{Gr}/A_T: graptolite area/total horizon area; A_{Gr}/A_{OM}: graptolite area/organic matter area.

3.2. TOC, Maceral, and Reflectance of Graptolite

The samples were crushed to 80 mesh size and treated in a sterilized crucible with 12.5% HCl to eliminate carbonates, then washed with distilled water every half an hour for three days. The oven-dried samples were measured using a Leco CS230 analyzer. The maceral and graptolite reflectance were performed in State Key Laboratory of Petroleum Resources and Prospecting, China University of Petroleum (Beijing). Firstly, 22 samples rich in graptolites were selected and cut into those with both length and width of 2 cm. Each of the samples was put into the plastic injection mold. The mixture of epoxy resin and coagulant (volume ratio is 5:2) was poured into the mold to cement at room temperature. Then, the samples were polished using a Buehler automatic grinding and polishing machine (EcoMet 250 with AutoMet 250) to obtain a smooth surface for the microscopic examination [2]. The optical characteristics and reflectance of the sample were performed using a 10-× eyepiece and a 50-× oil-immersion objective lens under reflected light at 546 nm wavelength (1.518 refractive index oil) using a Leica 4500 P microscope equipped with a CRAIC microscope photometer. The reflectance of the sample was measured at a room temperature of 22~24 °C with standards of known reflectance (Yttrium Aluminum Garnet, R_o = 1.72% and cubic zirconia, R_o = 3.08%).

3.3. SEM Observation of Graptolite

Samples were separately subjected to mechanical cutting, sandpaper polishing, and argon ion polishing with a voltage of 5.5 kV and a current of 2.1 mA (switching voltage and the current to 5.0 kV and 2.0 mA, respectively, every 30 min) to finish SEM sample preparation. In view of the fact that it is hard to observe graptolite organic matter in SEM images, the prepared polished SEM samples were observed under an optical microscope with a 10-× eyepiece and 50-× dry objective lens to investigate organic maceral (graptolite and solid bitumen). Graptolites are calibrated using the objective lens with a carving knife so that graptolite organic matter can be quickly and accurately observed under the SEM. The SEM sample preparation and observation were carried out in the Institute of Geology and Geophysics, Chinese Academy of Sciences, Beijing, China.

4. Results and Discussion

4.1. Total Organic Carbon Contents and Mineralogy of Graptolite-Bearing Shales

The TOC values of the shales from the Longmaxi Formation range from 0.40% to 3.62% with an average of 2.02%. The TOC values of the shale samples from XK1 to XK13 are below 2.0%, while the samples from XK14 to XK27 have higher TOC values over 2.0% (Table 1). Thus, organic-rich shales (TOC > 2.0%, XH14~XH27) and organic-bearing shales (TOC < 2.0%, XH1~XH13) can be divided according to the TOC value of 2.0%. Organic-rich shales have high contents of quartz and low contents of clay mineral, ranging from 48.3% to 79.4% and 16.2% to 32.9% (Table 1), respectively, with an average of 65.7% and 22.9%, respectively. The content of solid bitumen rather than graptolite is dominant in these shales (Table 1, Figure 2). However, organic-bearing shales have the opposite characteristics, with quartz and clay contents ranging from 34.7% to 61.5% and 25.2% to 51.7% (Table 1), respectively, with a mean value of 45.9% and 39.9% (Table 1), respectively. The content of graptolite dominates in these shales (Table 1, Figure 2). The high content of quartz in the organic-rich shales may be associated with high marine productivity [16]. All the samples have low contents of feldspar, ranging from 2.3% to 8.1% (Table 1). Pyrite is present in most organic-rich shale samples, while only six shale samples contain pyrite in the organic-bearing shales (Table 1).
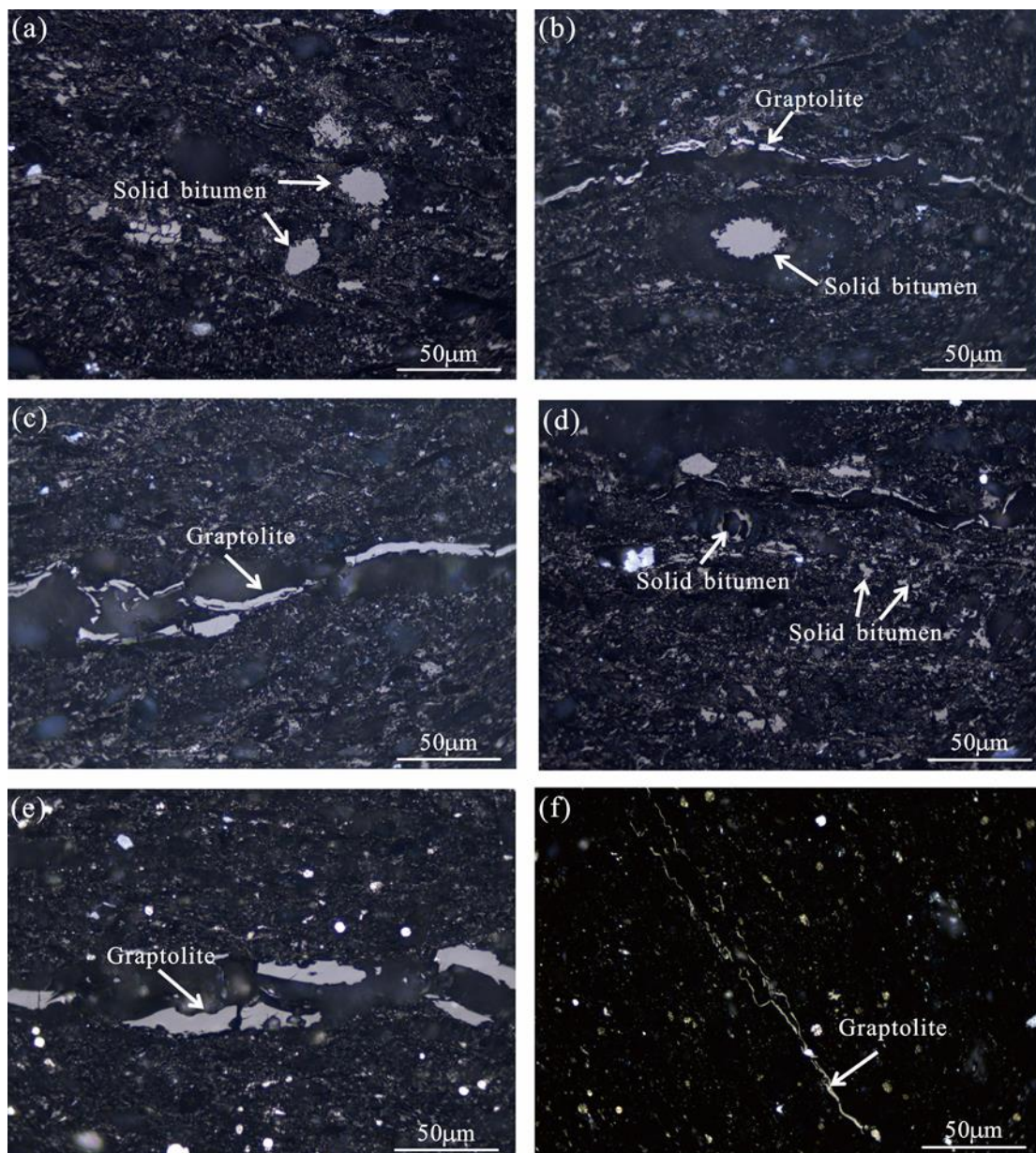
Table 1. TOC values and mineralogical composition of the shales in the Longmaxi Formation.

Sample No.	Depth (m)	TOC (%)	Mineral Composition						A_B/A_T (%)	A_{Gr}/A_T (%)	A_{Gr}/A_{OM} (%)
			Quartz (wt%)	Feldspar (wt%)	Carbonate Minerals (wt%)	Pyrite (wt%)	Clay (wt%)	Other Minerals (wt%)			
XK1	3.69	1.49	42.3	7.0	0	0	42.5	8.2	15.20	15.99	51.27
XK2	6.46	0.40	43.3	6.8	0	0	46.4	3.4	/	/	/
XK3	11.08	0.55	39.3	7.9	0	0	43.0	9.8	/	/	/
XK4	14.78	1.73	39.6	7.0	0	0	41.3	12.2	/	/	/
XK5	19.40	1.09	41.4	7.7	0	0	48.3	2.7	12.70	11.37	47.24
XK6	22.17	1.37	58.6	8.1	0	0	33.4	0	/	/	/
XK7	25.87	0.65	38.2	7.1	0	0	51.7	3.1	/	/	/
XK8	29.57	0.78	40.5	7.5	0	1.0	41.2	9.8	/	/	/
XK9	32.34	0.91	47.9	6.7	0	1.0	36.6	7.8	26.26	15.11	36.52
XK10	36.04	1.96	34.7	7.4	0	3.7	48.2	6.0	13.64	14.69	51.85
XK11	39.67	1.98	61.5	6.4	3.3	3.6	25.2	0	/	/	/
XK12	42.25	1.09	54.7	7.1	0	5.1	28.5	4.6	/	/	/
XK13	46.56	1.91	55.2	5.5	0	3.6	31.8	3.9	/	/	/
XK14	49.14	2.17	61.1	5.9	0	5.2	24.3	3.5	12.63	11.95	48.63
XK15	52.61	2.29	60.5	6.1	0	6.1	24.1	3.2	36.79	12.51	25.38
XK16	55.29	2.34	61.4	6.3	4.5	5.6	22.2	0	/	/	/
XK17	57.96	2.53	48.3	5.2	5.1	5.6	32.9	2.9	/	/	/
XK18	60.64	2.79	70.8	5.3	0	2.8	17.7	3.5	45.65	8.62	15.88
XK19	65.27	2.75	59.4	7.1	0	2.0	26.8	4.7	/	/	/
XK20	68.05	2.58	73.1	4.9	0	3.5	18.5	0	30.05	10.95	26.71
XK21	70.83	3.06	71.9	2.8	3.7	0	16.2	3.3	/	/	/
XK22	73.33	2.75	61.4	7.1	0	2.6	24.3	4.7	23.83	10.17	29.91
XK23	74.12	2.82	71.7	5.6	4.3	0	18.4	0	24.23	7.86	24.49
XK24	75.70	3.02	65.3	6.1	0	3.2	25.4	0	/	/	/
XK25	78.06	3.34	60.4	4.3	0	0	30.0	5.2	/	/	/
XK26	80.42	3.62	75.0	2.3	0	0	22.7	0	43.23	8.04	15.68
XK27	82.78	2.49	79.4	3.1	0	0	17.5	0	26.95	6.29	18.93

4.2. Maceral Characteristics of Graptolite-Derived Organic Matter

The organic matter of the Longmaxi shales is mainly from algae, bacteria, zooclast (graptolite, chitinozoans, sponge spicule), and acritarch [13]. Among the zooclast, graptolite is a significant source of organic matter in the Lower Paleozoic source rocks [17]. There is a positive relationship between TOC and the content of graptolite, which is significant to shale gas accumulation [18].

The graptolites and solid bitumen are the predominant macerals in the shales of the Longmaxi Formation in this study area. The solid bitumen shows sphericity or an ellipse with flattening or jagged edge, the surface of which is smooth under an oil-immersion objective using reflected light, and solid bitumen can be filled by siliceous minerals (Figure 3a,b,d). The graptolite epidermis in the Lower Paleozoic sediments shows two types of morphology under reflected light: granular and non-granular [2,19]. The graptolites of the Longmaxi shales in the study area exhibit non-granular characteristics. The well-preserved graptolite epidermis can be observed under reflected light showing tabular and laminar, which is intermittent and articulatory. The presence of fusellar layers of graptolites under polarized light can be observed in some samples. Graptolite epidermis shows anisotropic due to high organic matter maturity and is commonly filled by pyrites (Figure 3b,c,e,f). Graptolites are rich both in organic-bearing shales and organic-rich shales, while solid bitumen dominates in organic-rich shales.

Figure 3. Photomicrographs showing the organic components of the Longmaxi shales. (**a**), XH-27, solid bitumen; (**b**) XH-25, solid bitumen and non-granular graptolites; (**c**) XH-25, non-granular graptolites; (**d**) XH-27, solid bitumen; (**e**) XH-13, non-granular graptolites; (**f**) XH-9, non-granular graptolites.

4.3. The Reflectance of Graptolite

It is hard to evaluate the organic matter maturity of the Lower Paleozoic source rocks due to the lack of vitrinite. Some scholars found that some vitrinite-like macerals, such as graptolite, chitinozoans, and solid bitumen, could be used to evaluate organic matter maturity of the Lower Paleozoic marine source rocks [20–29]. The reflectance of graptolites has been widely investigated [2,28,30,31], showing that graptolite has anisotropy and the reflectance of graptolite changes regularly with the increase of the organic matter maturity, which can be an indicator of organic matter maturity of the Ordovician and Silurian source rocks.

A total of 17 graptolite-bearing shale samples were collected for random reflectance of graptolite examination. The equivalent vitrinite reflectance can be obtained according to the formula proposed by Cao et al. [23]. The random reflectance of graptolites ranges from

4.43% to 5.43% (Table 2), and the calculated equivalent vitrinite reflectance is in the range from 2.46% to 2.76% (Table 2) with the average of 2.68%. It suggests that organic matter maturity of the Longmaxi shales in the study area is overmature.

Table 2. Distribution characteristics of the reflectance of graptolites and equivalent vitrinite of the Longmaxi shales.
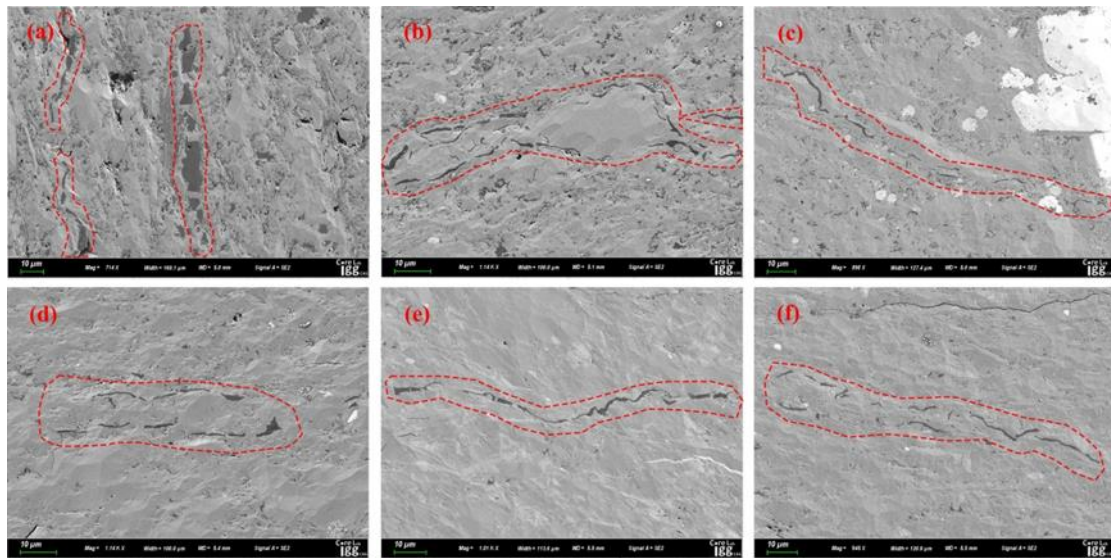
Sample No.	GR_{ran}, %	$EqVR_o$, %
XH-27	4.43	2.46
XH-26	5.53	2.73
XH-25	5.43	2.76
XH-23	5.35	2.74
XH-21	5.20	2.70
XH-20	5.22	2.70
XH-19	5.07	2.66
XH-18	5.09	2.66
XH-17	5.36	2.74
XH-15	5.35	2.74
XH-13	5.37	2.75
XH-10	5.08	2.66
XH-9	5.06	2.65
XH-6	5.28	2.72
XH-4	5.12	2.67
XH-1	4.85	2.59

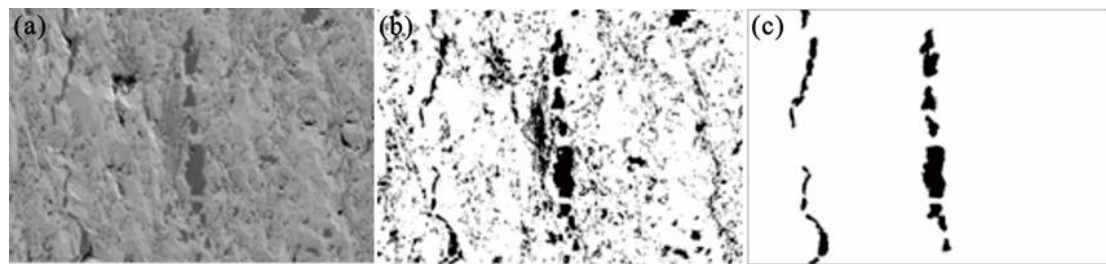*4.4. Contribution of Graptolites to Buried Organic Carbon*

The components of organic matter, such as graptolite and solid bitumen, are hard to distinguish under the SEM. To overcome the above problem, the prepared polished SEM samples were observed under an optical microscope to distinguish organic maceral. Graptolites were calibrated using the objective lens with a carving knife so that graptolite organic matter can be quickly and accurately observed under the SEM (Figure 4a–f). The SEM images of 12 samples were chosen to discuss the contribution of graptolites to buried organic carbon. The area of graptolites and organic matter can be extracted through threshold segmentation using Image J software, and the results can be calculated (Figure 5, Table 3). We chose many images of each sample to ensure the reliability of the results (Table 3 only exhibits one image processing result in each sample). Thus, the average ratio of the areal contribution rate of graptolite (proportion of graptolite area to organic matter area) in each sample can be obtained, ranging from 15.68% to 51.85% (Figure 6), and the average ratio of A_{GR}/A_{OM} is up to 32.71%.

There is a negative correlation between the TOC value of the organic-rich shales and the areal contribution rate of graptolite (Figure 6), suggesting that solid bitumen rather than graptolite mainly contributes to buried organic carbon of the organic-rich shales in the Longmaxi Formation. However, the TOC value of organic-bearing shales has a positive correlation with the areal contribution rate of graptolites (Figure 6), indicating that graptolites are the main contributor to buried organic carbon. The solid bitumen in the organic-bearing shales is relatively undeveloped, and the contribution of graptolites to buried organic carbon is highlighted.
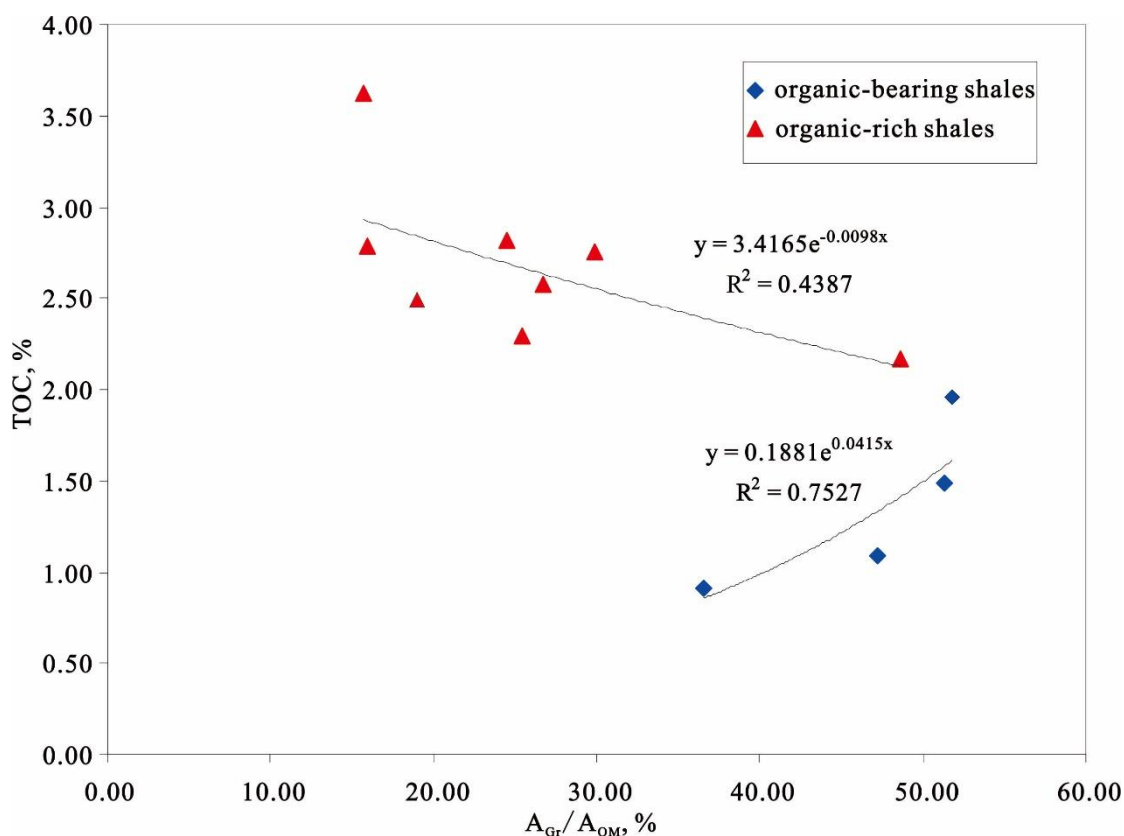
Figure 4. SEM images of the graptolites in the Longmaxi shales: (**a**), XH-27, length = 160.1 μm; (**b**), XH-23, length = 100.0 μm; (**c**) XH-15, length = 127.4 μm; (**d**), XH-9, length = 100.0 μm; (**e**), XH-5, length = 113.6 μm; (**f**), XH-1, length = 120.9 μm.

Figure 5. Graptolite area extraction steps by SEM images. (**a**), primary SEM image; (**b**), binary image; (**c**) graptolite area extraction.

Table 3. Distribution characteristics of the area of graptolite and organic matter in the Longmaxi shales.

Sample No.	A_{Gr}	A_{OM}
XK-27	251.77	1329.83
XK-26	88.44	563.96
XK-23	121.8	497.34
XK-22	160.68	537.25
XK-20	186.18	697.08
XK-18	189.58	1193.80
XK-15	45.04	177.49
XK-14	179.31	368.71
XK-10	367.19	708.22
XK-9	90.65	248.22
XK-5	54.59	115.55
XK-1	95.94	187.13

Figure 6. Correlation between the areal contribution rate of graptolites and TOC value. A_{Gr}, graptolite area; A_{OM}, area of organic matter.

5. Conclusions

Shales in the Longmaxi Formation can be divided into organic-rich shales (TOC > 2.0%) and organic-bearing shales (TOC < 2.0%). The organic-rich shales have high quartz content and low clay mineral content, while that in the organic-bearing shales is opposite.

Solid bitumen and graptolites are the main organic components in the Longmaxi shales, and graptolite is widely distributed both in the organic-rich and organic-bearing shales, while the former commonly exists in the organic-rich shales. The equivalent vitrinite reflectance calculated by the reflectance of graptolite ranges from 2.46% to 2.76%, suggesting overmaturity of the organic matter of the shales.

The proportion of graptolite area to organic matter area is relatively large. Solid bitumen mainly contributes to buried organic carbon of the organic-rich shales in the Longmaxi Formation, while the graptolites are the dominant contributor to buried organic carbon of the organic-bearing shales.

References

1. Luo, Q.Y.; Zhong, N.N.; Dai, N.; Zhang, W. Graptolite-derived organic matter in the Wufeng-Longmaxi Formations (Upper Ordovician-Lower Silurian) of southeastern Chongqing, China: Implications for gas shale evaluation. *Int. J. Coal Geol.* **2016**, *153*, 87–98. [CrossRef]
2. Luo, Q.Y.; Hao, J.Y.; Skovsted, C.B.; Xu, Y.H.; Liu, Y.; Wu, J.; Zhang, S.N.; Wang, W.L. Optical characteristics of graptolite-bearing sediments and its implication for thermal maturity assessment. *Int. J. Coal Geol.* **2018**, *195*, 386–401. [CrossRef]
3. Gong, J.M.; Qiu, Z.; Zou, C.N.; Wang, H.Y.; Shi, Z.S. An integrated assessment system for shale gas resources associated with graptolites and its application. *Appl. Energy* **2020**, *262*, 114524. [CrossRef]
4. Meng, M.M.; Ge, H.K.; Shen, Y.H.; Ji, W.M. Fractal characterization of pore structure and its influence on salt ion diffusion behavior in marine shale reservoirs. *Int. J. Hydrogen Energy* **2020**, *45*, 28520–28530. [CrossRef]
5. Han, H.; Cao, Y.; Chen, S.J.; Lu, J.G.; Huang, C.X.; Zhu, H.H.; Zhan, P.; Gao, Y. Influence of particle size on gas-adsorption experiments of shales: An example from a Longmaxi Shale sample from the Sichuan Basin, China. *Fuel* **2016**, *186*, 750–757. [CrossRef]
6. Fan, J.X.; Melchin, M.J.; Chen, X.; Wang, Y.; Zhang, Y.D.; Chen, Q.; Chi, Z.L.; Chen, F. Biostratigraphy and geography of the Ordovician-Silurian Lungmachi black shales in South China. *Sci. China Earth Sci.* **2011**, *54*, 1854–1863. [CrossRef]
7. Gorjan, P.; Kaiho, K.; Fike, D.A.; Chen, X. Carbon-and sulfur-isotope geochemistry of the Hirnantian (Late Ordovician) Wangji-awan (Riverside) section, South China: Global correlation and environmental event interpretation. *Palaeogeogr. Palaeoclimatol. Palaeoecol.* **2012**, *337–338*, 14–22. [CrossRef]
8. Chen, X.; Chen, Q.; Aung, K.P.; Muir, L.A. Latest Ordovician graptolites from the Mandalay Region, Myanmar. *Palaeoworld* **2020**, *29*, 47–65. [CrossRef]
9. Yan, C.N.; Jin, Z.J.; Zhao, J.H.; Du, W.; Liu, Q.Y. Influence of sedimentary environment on organic matter enrichment in shale: A case study of the Wufeng and Longmaxi Formations of the Sichuan Basin, China. *Mar. Pet. Geol.* **2018**, *92*, 880–894. [CrossRef]
10. Zhang, Y.Y.; He, Z.L.; Lu, S.F.; Jiang, S.; Xiao, D.S.; Long, S.X.; Gao, B.; Du, W.; Zhao, J.H.; Chen, G.H.; et al. Characteristics of microorganisms and origin of organic matter in Wufeng Formation and Longmaxi Formation in Sichuan Basin, South China. *Mar. Pet. Geol.* **2020**, *111*, 363–374. [CrossRef]
11. Jin, S.D.; Deng, H.C.; Zhu, X.; Liu, Y.; Liu, S.B.; Fu, M.Y. Orbital control on cyclical organic matter accumulation in Early Silurian Longmaxi Formation shales. *Geosci. Front.* **2020**, *11*, 533–545. [CrossRef]
12. Liu, D.M.; Hou, X.Q.; Jiang, J.P. The composition and structure of graptolite—A micro-area analysis. *Acta Mineral. Sin.* **1996**, *16*, 53–57. (In Chinese with English Abstract)
13. Borjigin, T.; Shen, B.J.; Yu, L.J.; Yang, Y.F.; Zhang, W.T.; Tao, C.; Xi, B.B.; Zhang, Q.Z.; Bao, F.; Qin, J.Z. Mechanims of shale gas generation and accumulation in the Ordovician Wufeng-Longmaxi Formation, Sichuan Basin, SW China. *Pet. Explor. Dev.* **2017**, *44*, 69–78. [CrossRef]
14. Ma, Y.; Zhong, N.N.; Cheng, L.J.; Pan, Z.J.; Dai, N.; Zhang, Y.; Yang, L. Pore structure of the graptolite-derived OM in the Longmaxi shale, southeastern Upper Yangtze Region, China. *Mar. Pet. Geol.* **2016**, *72*, 1–11. [CrossRef]
15. Stockey, R.G.; Cole, D.B.; Planavsky, N.J.; Loydell, D.K.; Fryda, J.; Sperling, E.A. Persistent global marine euxinia in the early Silurian. *Nat. Commun.* **2020**, *11*, 1804. [CrossRef] [PubMed]
16. Zhao, J.H.; Jin, Z.K.; Jin, Z.J.; Wen, X.; Geng, Y.K. Origin of authigenic quartz in organic-rich shales of the Wufeng and Longmaxi Formations in the Sichuan Basin, South China: Implications for pore evolution. *J. Nat. Gas Sci. Eng.* **2017**, *38*, 21–38. [CrossRef]
17. Deng, K.; Zhou, W.; Zhou, L.F.; Wan, Y.Z.; Deng, H.C.; Xie, R.C.; Chen, W.L. Influencing factors of micropores in the graptolite shale of Ordovician Pingliang Formation in Ordos Basin, NW China. *Pet. Explor. Dev.* **2016**, *43*, 416–424. [CrossRef]
18. Petersen, H.I.; Schovsbon, H.; Nielsen, A.T. Reflectance measurements of zooclasts and solid bitumen in Lower Palaeozoic shales, southern Scandinavia: Correlation to vitrinite reflectance. *Int. J. Coal Geol.* **2013**, *114*, 1–18. [CrossRef]
19. Goodarzi, F.; Norford, B.S. Graptolites as indicators of the temperature histories of rocks. *J. Geol. Soc.* **1985**, *142*, 1089–1099. [CrossRef]
20. Bertrand, R. Correlations among the reflectances of vitrinite, chitinozoans, graptolites and scolecodonts. *Org. Geochem.* **1990**, *15*, 565–574. [CrossRef]
21. Bertrand, R. Standardization of solid bitumen reflectance to vitrinite in some Paleozoic sequences of Canada. *Energy Sources* **1993**, *15*, 269–287. [CrossRef]
22. Gentzis, T.; de Freitas, T.; Goodarzi, F.; Melchin, M.; Lenz, A. Thermal maturity of Lower Paleozoic sedimentary successions in Arctic Canada. *AAPG Bull.* **1996**, *80*, 1065–1083.
23. Cao, C.Q.; Shang, Q.H.; Fang, Y.T. The study of graptolite reflectance as the indicator of source-rock maturation in Ordovician and Silurian of Tarim Basin, Ordos, Jiangsu Areas. *Acta Palaeontol. Sin.* **2000**, *39*, 151–156, (In Chinese with English Abstract).
24. Suárez-Ruiz, I.; Flores, D.; Mendonça Filho, J.G.; Hackley, P.C. Review and update of the applications of organic petrology: Part 1, geological applications. *Int. J. Coal Geol.* **2012**, *99*, 54–112. [CrossRef]
25. İnan, S.; Goodarzi, F.; Mumm, A.S.; Arouri, K.; Qathami, S.; Ardakani, O.H.; İnan, T.; Tuwailib, A.A. The Silurian Qusaiba Hot Shales of Saudi Arabia: An integrated assessment of thermal maturity. *Int. J. Coal Geol.* **2016**, *159*, 107–119. [CrossRef]
26. Lavoie, D.; Pinet, N.; Bordeleau, G.; Ardakani, O.H.; Ladevèze, P.; Duchesne, M.J.; Rivard, C.; Mort, A.; Brake, V.; Sanei, H. The Upper Ordovician black shales of southern Quebec (Canada) and their significance for naturally occurring hydrocarbons in shallow groundwater. *Int. J. Coal Geol.* **2016**, *158*, 44–64. [CrossRef]

27. Luo, Q.Y.; Hao, J.; Skovsted, C.B.; Luo, P.; Khan, I.; Wu, J.; Zhong, N.N. The organic petrology of graptolites and maturity assessment of the Wufeng–Longmaxi Formations from Chongqing, China: Insights from reflectance cross-plot analysis. *Int. J. Coal Geol.* **2017**, *183*, 161–173. [CrossRef]

28. Luo, Q.Y.; Fariborz, G.; Zhong, N.N.; Wang, Y.; Qiu, N.S.; Skovsted, C.B.; Suchý, V.; Schovsbo, N.H.; Morga, R.; Xu, Y.H.; et al. Graptolites as fossil geo-thermometers and source material of hydrocarbons: An overview of four decades of progress. *Earth-Sci. Rev.* **2020**, *200*, 103000. [CrossRef]

29. Schmidt, J.S.; Menezes, T.R.; Souza, I.V.A.F.; Spigolon, A.L.D.; Pestilho, A.L.S.; Coutinho, L.F.C. Comments on empirical conversion of solid bitumen reflectance for thermal maturity evaluation. *Int. J. Coal Geol.* **2019**, *201*, 44–50. [CrossRef]

30. Bertrand, R.; Malo, M. Source rock analysis, thermal maturation and hydrocarbon generation in Siluro-Devonian rocks of the Gaspé Belt basin, Canada. *Bull. Can. Pet. Geol.* **2001**, *49*, 238–261. [CrossRef]

31. Bertrand, R.; Lavoie, D.; Fowler, M. Cambrian-Ordovician shales in the Humber zone: Thermal maturation and source rock potential. *Bull. Can. Pet. Geol.* **2003**, *51*, 213–233. [CrossRef]